

# Modeling A Scalable High-Speed Interconnect with Stochastic Petri Nets

Gianfranco Ciardo\*

Department of Computer Science  
College of William and Mary,  
Williamsburg, VA 23187-8795, USA  
ciardo@cs.wm.edu

Lucy Cherkasova, Vadim Kotov, Tom Rokicki

Hewlett-Packard Laboratories  
1501 Page Mill Road  
Palo Alto, CA 94303, USA  
{cherkasova,kotov,rokicki}@hpl.hp.com

## Abstract

*This paper presents an approach to using Stochastic Petri nets to model large-scale concurrent systems, in our case, a scalable computer interconnect. We show how Stochastic Petri net models can exploit the symmetry of the system to construct a tractable, but approximate, analytic model, and that they can yield results very close to those of a detailed simulation model, with much less computational effort.*

## 1 Introduction

In this paper, we present techniques for the modeling and analysis of large-scale concurrent systems using Petri nets. There are two important but conflicting requirements in this sort of analysis. First, the model should be detailed enough to include those system features that have a significant impact on performance. Second, the model should be simple enough to be tractable. Constructing a single model of a complex system does not lead to completely trustworthy results; modeling is subject to the same sorts of errors and inaccuracies as programming in general, yet the results are often not as easy to check. We therefore use different types of models to deal with different aspects and stages of the system analysis. The common feature of these models is that they are based on Petri nets.

We present as a case study the net modeling of a *scalable interconnect* for its performance evaluation and analysis. Our goal was to analyze the performance of the interconnect as a function of various parameters, including network size (which can scale up to hundreds of nodes) and the number of internal buffers on each node.

We have built and analyzed two net models of the interconnect. We used SPNP [6], based on *Stochastic Petri Nets* (SPNs), to build an approximate model for a quick numerical analysis of performance. We used Design/CPN<sup>TM</sup>

[7] based on *Hierarchical Colored Petri Nets* to develop a detailed simulation model to help refine the design and identify performance bottlenecks. This model was also used to verify the accuracy and correctness of the approximate SPN model.

The original Petri net formalism is inadequate for the specification of complex large-scale systems, especially systems for which the number of interacting components depends on the input parameters. We instead use two higher-level formalisms based on Petri nets.

High level Petri nets, in particular Colored Petri nets, provide for the specification of large-scale systems with colored tokens, that allow the folding of the system description into a very compact form. The Colored Petri nets used in Design/CPN are a graphical programming language with rich specification and simulation possibilities. The colored tokens and arc expressions allow easy parameterization of the system size. Through the use of hierarchy and refinement, a series of models with different levels of detail can be easily constructed, enabling rapid prototyping and analysis. The main difficulty when modeling complex systems with high level Petri nets is that the simulation time of these nets does not remain constant with increasing system size. For a very large number of components, simulation time becomes prohibitive.

SPNs allow the quick construction of a simplified abstract model that is then numerically solved for different model parameters. This analysis is based on the exploration of all reachable states in the model, and is thus even more dependent on the system size. A straightforward SPN model of the interconnect generates exceedingly large stochastic processes for even the smallest network sizes.

The solution to this problem is to construct an approximate model that takes into the consideration some specific features of the modeled system. In our case, we exploit the fact that the interconnect has a very regular structure. We were primarily concerned with two different issues:

---

\* This research was initiated while G. Ciardo was visiting Hewlett-Packard Labs.

- 1) how performance scales with network size, and
- 2) how internal design alternatives affect performance.

These tasks are not independent of one another. Nonetheless, it is possible to split the problem into two stages. First, a simplified but scalable model to predict bottom-line performance and identify possible bottlenecks is quickly constructed. Next, a detailed model is constructed to evaluate and analyze particular design alternatives. These two stages may be iterated to verify the results and refine the analysis.

In this paper, we show how SPNs can exploit the symmetry of the system to construct a tractable approximate model. We present this model to support our conclusion that SPNs can be successfully used for modeling industrial size systems. Sections 2 and 3 present the interconnect structure and its exact SPN model. Section 4 presents our approach to build a tractable approximate SPN model. Section 5 presents the numerical results. Section 6 compares the numerical results of SPN model with simulation results of the interconnect model based on Colored Petri nets. In the conclusion, we discuss a few missing features of SPNP which might further improve the applicability of such a tool.

We assume that the reader is familiar with the basic definitions and behavior of SPNs. For a complete treatment of the class of SPNs used in this paper, see [3].

## 2 System

The interconnect topology is a continuous hexagonal mesh which permits each node to communicate with its six immediate neighbors. We refer to a mesh having  $n$  nodes on each edge as an  $E_n$  mesh. The resulting total number of nodes is  $N = 3n(n - 1) + 1$ . Figure 1 shows the mesh structure for  $E_2$ ,  $E_3$ , and  $E_4$ . Physically, nodes on the edge are actually connected to nodes on other edges in a wraparound fashion, so that their virtual connectivity is the same as that of internal nodes.

The distance of a node from a particular node  $i$  in an  $E_n$  mesh is at most  $n - 1$  ‘‘hops’’. Furthermore, of the  $N - 1 = 3n(n - 1)$  nodes other than  $i$ , 6 are at distance 1, 12 are at distance 2, and so on, up to the  $6(n - 1)$  at distance  $n - 1$ .

Each node is attached to a processor connected via a local bidirectional port. In addition, each node  $i$  has six ports, numbered 0 through 5, each of them connecting it to a different neighbor,  $n(i, 0)$  through  $n(i, 5)$ , respectively (see Figure 2). Each of these ports is full-duplex.

The node has a total of  $N_b$  buffers to store the packets in transit. The processor injects packets to the interconnect through the local ports when both 1) the local port is available and 2) there is an available buffer to store the packet. Otherwise, the packet waits in a queue until the required

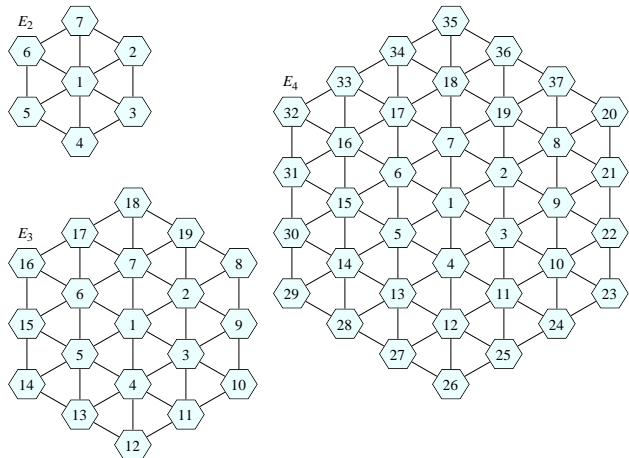


Figure 1: System structure, for  $n = 2, 3,$  and  $4$ .

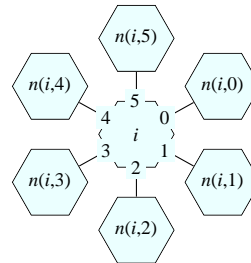


Figure 2: Neighbor nodes.

resources are freed. In-transit packets follow the same procedure. Packets are always routed through a minimal-length path towards their destination. Each time the packet

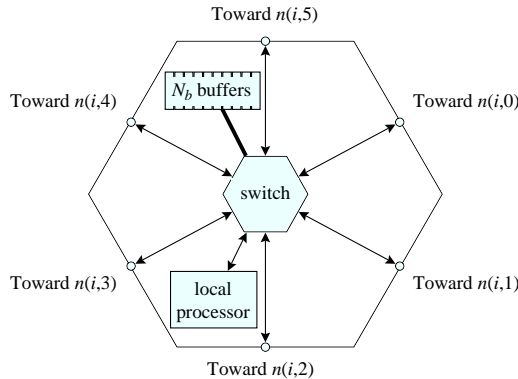


Figure 3: Node structure.

arrives at a new node, the next node on a minimal path to destination is computed and the router attempts to forward the packet through it. If either the port is busy or no buffers in the next node are available, the packet waits. When the packet finally arrives to a destination node, it is ejected from the interconnect through the local processor port.

We assume packet transfer, injection, or ejection takes  $720 tu$  (time units). A main parameter of the model is the number of buffers inside each node; we use a default of ten.

### 3 Detailed model

A detailed SPN model for node  $i$  is shown in Figure 4. Transition  $Generate^i$  generates the packet tokens at a given rate and puts them into place  $Wait^i$ . Place  $EB^i$  contains tokens corresponding to empty buffers inside node  $i$ . The number of tokens  $N_b$  initially in this place is the total number of buffers in node  $i$ .

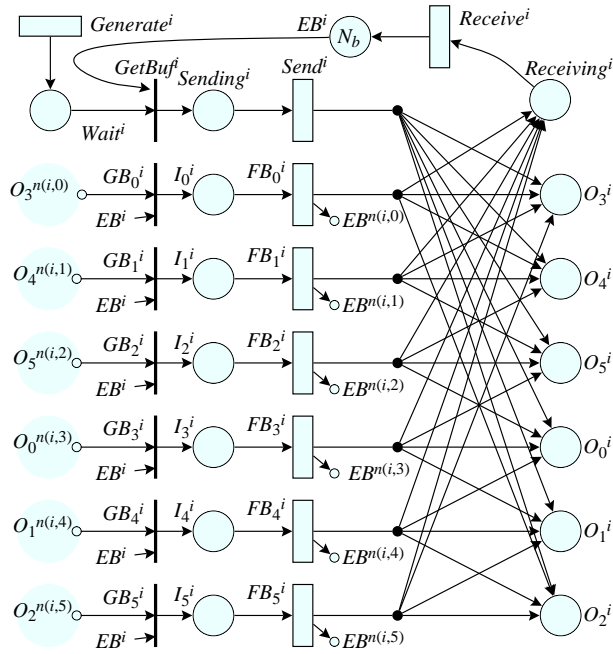


Figure 4: Detailed SPN model.

Firing of the immediate transition  $GetBuf^i$  reserves a buffer inside node  $i$  (if there is a token in place  $EB^i$ ) for the new packet and moves a token to place  $Sending^i$ . The packet injection to node  $i$  is represented by transition  $Send^i$ .

The output places  $O_0^i, \dots, O_5^i$  of node  $i$  are the input places for the six neighbor nodes: for example, place  $O_3^i$  is the input place for node  $n(i, 3)$  from node  $i$ .

For simplicity of illustration, a “probabilistic arc” is used from transition  $Send^i$  to places  $O_0^i$  through  $O_5^i$ . A proba-

bilistic arc is a shorthand to denote that the token deposited by a transition, say  $Send^i$ , can end up in exactly one of the destination places. Formally, this behavior is obtained with one extra place and a set of immediate transitions. For the branches from  $Send^i$  to  $O_0^i$  through  $O_5^i$ , we specify a probability of  $1/6$ , since we assume that the destination node for a packet generated at node  $i$  is uniformly chosen among the remaining nodes.

The packets arrive to each node from the local processor (through the local port) and from the six neighbor nodes (through neighbor ports). Places with a superscript  $n(i, 0)$  through  $n(i, 5)$  are in the individual SPNs representing the six neighbor nodes. They are drawn smaller for clarity. For example, place  $O_3^{n(i,0)}$  is the place in the SPN for the neighbor  $n(i, 0)$  of  $i$ .

The packet transfer from the neighbor nodes is the same as from the local processor. First of all, for each packet arriving at node  $i$ , a buffer must be reserved. Firing of immediate transition  $GB_j^i$ , ( $j = 0, \dots, 5$ ) reserves the buffer inside node  $i$  if there is one available, represented by a token in place  $EB^i$ . The firing of transition  $FB_j^i$  corresponds to the packet transfer by the input port  $j$  to a node  $i$ . When the packet transfer is complete, the buffer occupied by this packet in the previous node  $n(i, j)$  is released by returning a token to place  $EB^{n(i,j)}$ .

A probabilistic arc is used from transitions  $FB_0^i$  through  $FB_5^i$  to places  $Receiving^i$  and  $O_0^i$  through  $O_5^i$ ; these are expanded into extra places and immediate transitions as described before. There are two possibilities:

1. If the packet is destined for node  $i$  then it is put in place  $Receiving^i$ , and ejected from the node by the local processor port (represented by transition  $Receive^i$ ). When the packet ejection is complete, one buffer is released by returning a token to place  $EB^i$ .
2. If the packet is intended for a neighbor node  $j$  then it is put into place  $O_j^i$ .

Assuming that packets are always routed through one of the shortest paths, a packet arriving from port  $j$  can only be sent to the current node (place  $Receiving^i$ ) or to another node to be reached through ports  $(j + 2) \bmod 6$ ,  $(j + 3) \bmod 6$ , or  $(j + 4) \bmod 6$ . That is, a packet never reverses direction. The routing probabilities depend on both the source and the destination of the packet. For  $E_2$ , external packets arriving at node  $i$  always have their destination as node  $i$ , since the maximum distance between any two nodes is one. When modeling  $E_n$ ,  $n > 2$ , we can associate the identity of the source and destination with each token representing a packet, resulting in a colored SPN with a huge state space.

Alternatively, we can remain in the uncolored domain and obtain considerable state space reduction by assigning probabilities to the four possible destinations for a packet arriving through port  $j$ :

- the local node,  $i$ , with probability  $p_{local}$ ,
- an external node reachable through port  $(j+2) \bmod 6$ , with probability  $p_{side}$ ,
- an external node reachable through port  $(j+3) \bmod 6$ , with probability  $p_{center}$ ,
- an external node reachable through port  $(j+4) \bmod 6$ , with probability  $p_{side}$  again, since, by symmetry, this case has the same probability as in the second case above.

This probabilistic view involves an approximation, since it is now possible to have packets follow arbitrarily long paths through the mesh. On the other hand, it is nevertheless possible to set the parameter  $p_{local}$  so that the average load on the network is correctly matched, and each port on each node has the same load. We define a “hop” to be the movement of a packet from a node to one of its neighbors, and compute the average number of hops required to send a packet from source to destination. For  $E_n$ , if node  $i$  sends to every other node with equal probability, then  $6k$  potential destinations out of  $3n(n-1)$  are  $k$  hops away, hence the average number of hops is

$$\sum_{k=1}^{n-1} k \cdot \frac{6k}{3n(n-1)} = \frac{2n-1}{3}$$

In particular, the average number of hops is 1 for  $E_2$ , as expected. Each incoming packet corresponds to one hop, hence a fraction

$$p_{local} = \left(\frac{2n-1}{3}\right)^{-1} = \frac{3}{2n-1}$$

of the incoming packets is directed to the local node  $i$ .

We stress that this choice for  $p_{local}$  ensures that the expected number of hops per packet and the average rate of hops over the entire mesh,  $N\lambda/p_{local}$ , or to an individual node,  $\lambda/p_{local}$ , or even to an individual port,  $1/6 \cdot \lambda/p_{local}$ , is the same for the exact colored model and for the approximate probabilistic model, where  $\lambda$  is the injection rate from each node. The only approximation lies in the probability mass function (pmf) of the number of hops for a packet. In the exact model,

$$\Pr\{\text{number of hops is } k\} = \frac{6k}{3n(n-1)},$$

while, in the approximate model,

$$\Pr\{\text{number of hops is } k\} = \frac{3}{2n-1} \left(1 - \frac{3}{2n-1}\right)^{k-1},$$

which describes a geometric distribution. The quality of approximation increases with the size  $n$  of the mesh, since

the number of nodes increases quadratically in  $n$ , while the expected number of hops increases linearly in  $n$ .

Clearly,  $p_{local} + p_{center} + 2p_{side} = 1$ , but  $p_{center}$  and  $p_{side}$  still need to be determined. Observing Fig. 1 again, this corresponds to determining the proportion of hops of type “ $l$ ”, “ $c$ ”, and “ $s$ ”, defined as the first hop (i.e., a packet from the local processor on node 1 exits on the port from 1 to 2), a hop going to the center port (i.e., a packet entered on the port from 1 to 2 exits on the port from 2 to 8), and a hop going to a side port (i.e., a packet entered on the port from 1 to 2 exits on the port from 2 to 9), respectively.

Define  $H_n$  to be the expected number of hops of the three types for a packet transmitted in  $E_n$ , starting from node 1 (because of the symmetric nature of the network, the choice of node 1 is arbitrary). For  $E_2$ , each packet takes exactly one hop of type  $l$ , hence  $H_2 = l$ . For  $E_3$ , each packet can take the following combinations of hops:

- From 1 to  $\{2, 3, \dots, 7\}$ : one hop of type  $l$ .
- From 1 to  $\{8, 10, \dots, 18\}$ : one hop of type  $l$  and one hop of type  $c$ .
- From 1 to  $\{9, 11, \dots, 19\}$ : one hop of type  $l$  and one hop of type  $s$ .

Assuming that each node other than 1 is a potential destination with equal probability,  $H_3 = l + \frac{1}{3}c + \frac{1}{3}s$ .

For larger size networks, the analysis becomes more complex. For example, in  $E_4$ , a packet with source node 1 and destination node 21 can choose among three paths:  $1 \xrightarrow{l} 2 \xrightarrow{c} 8 \xrightarrow{s} 21$ ,  $1 \xrightarrow{l} 2 \xrightarrow{s} 9 \xrightarrow{s} 21$ , and  $1 \xrightarrow{l} 3 \xrightarrow{s} 9 \xrightarrow{c} 21$ . For the analysis, we assume that, whenever a hop to either one of two neighbors would still achieve the shortest path for the packet, the choice is performed with uniform probability (e.g.,  $1 \xrightarrow{l} 2$  and  $1 \xrightarrow{l} 3$  have probability 1/2, and, given that  $1 \xrightarrow{l} 2$  is chosen,  $2 \xrightarrow{c} 8$  and  $2 \xrightarrow{c} 9$  have probability 1/2). Hence, the probability of the above three paths is 1/4, 1/4, and 1/2, respectively, not simply 1/3 for each of them. By enumerating these paths and computing their probabilities, we can then obtain  $H_4 = l + \frac{11}{12}c + \frac{5}{12}s$ . For  $E_5$ , we obtain  $H_5 = l + \frac{29}{20}c + \frac{11}{20}s$ . This implies that the value of  $p_{center}$  and  $p_{side}$  depends on the size of the network. However, their relative value will not affect the average load on the mesh, hence, we could, for simplicity, use the values

$$p_{center} = \frac{1 - p_{local}}{2} = \frac{n-2}{2n-1}$$

$$p_{side} = \frac{1 - p_{local}}{4} = \frac{n-2}{2(2n-1)},$$

which coincide with the exact values for  $n = 2, 3$ .

## 4 Approximate model

By assuming that the firing times of the timed transitions for the SPN in Fig. 4 are exponentially distributed, the resulting underlying stochastic process is a continuous-time Markov chain (CTMC). In principle, we could study this CTMC to compute the performance measures of interest using software tools such as SPNP [6], but its size is too large for an exact numerical solution, even for the  $E_2$  interconnect having only 7 nodes. In this section, we describe an approximate model based on the idea of SPN decomposition and fixed-point iteration [5]. This approximate model exploits the large amount of symmetry possessed by the interconnect and essentially describes the behavior of one node under a workload that is generated by the whole interconnect fabric. Thus the basic idea is to approximate and generate a proper amount of traffic going through one node in a network of a particular size.

We will construct the approximate SPN model from the following four SPN subnets representing different node activities from the perspective of a single “current” node:

1. Injection into the node by the local processor port.
2. Transfer from the current node to a neighbor node.
3. Transfer from the neighbor node to a current node.
4. Ejection from the current node to a processor by the local processor port.

**SPN subnet  $\mathcal{N}_1$**  is shown in Figure 5. Transition  $A_l$  generates the packets at a given rate  $\lambda$  and puts them in place  $WB_l$ . An inhibitor arc with cardinality  $K_l$  from  $WB_l$  to  $A_l$  is needed to ensure that the population of packets waiting to enter the node from the current node is finite. If  $K_l$  is smaller than the actual theoretical maximum number of packets waiting to enter the node from the local node, the inhibitor arc introduces an approximation through truncation of the state space.

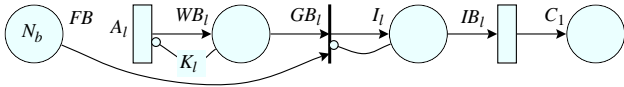


Figure 5: SPN subnet  $\mathcal{N}_1$ : packet injection into a node by the local processor port.

Place  $FB$  contains tokens corresponding to free buffers inside the current node. The initial number of tokens  $N_b$  is the total number of buffers in a node. The immediate transition  $GB_l$  reserves a buffer, if one is available (indicated by a token in place  $FB$ ). An inhibitor arc from place  $I_l$  to transition  $GB_l$  insures that the local processor port is not already busy (indicated by a token waiting in  $I_l$ ). After  $IB_l$

fires, the token is put into place  $C_1$  which is shared with subnet  $\mathcal{N}_2$ .

Tokens in place  $C_1$  represent packets stored in the current node buffers and which must be transferred to neighbor nodes.

**SPN subnet  $\mathcal{N}_2$**  is shown in Figure 6. Place  $FOP$  contains tokens corresponding to free output ports of the current node to its neighbor nodes. The initial number of tokens in  $FOP$  is six, since there are six neighbor nodes. When a token arrives in place  $C_1$ , either

- the required output port is available, immediate transition  $OPY_1$  fires, and the token is moved to place  $O_e$ , or
- the required output port is busy, immediate transition  $OPN_1$  fires, and the token is moved to place  $WOP$ . An inhibitor arc with cardinality six from  $FOP$  to  $OPN_1$  prevents transition  $OPN_1$  from firing when place  $FOP$  contains all six tokens.

Let  $\#(p)$  denote the number of tokens in place  $p$ . Then, the probability that a particular output port is free is  $\#(FOP)/6$ , and is assigned to transition  $OPY_1$ , while transition  $OPN_1$  is assigned a probability of  $1 - \#(FOP)/6$ .

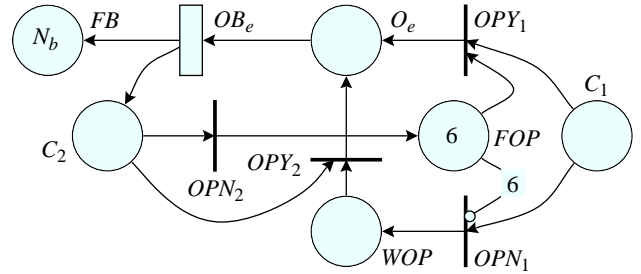


Figure 6: SPN subnet  $\mathcal{N}_2$ : packet transfer from the current node to its neighbor nodes.

Tokens in place  $O_e$  represent packets being transferred through output ports, and transition  $OB_e$  represents the completion of the packet transfer. Its rate is proportional to  $\#(O_e)$ , an “infinite server” behavior. When the packet transfer to a neighbor node is completed, a buffer is released by returning a token to place  $FB$ . Place  $C_2$  represents the state when the busy output port has just been released. There are two possibilities at this point. Either

- place  $WOP$  has a packet waiting for this particular output port, in which case transition  $OPY_2$  will fire, removing a token from  $WOP$ , or
- there is no waiting packet for this output port, in which case immediate transition  $OPN_2$  will fire, adding a token to  $FOP$ .

Let us calculate the probability that there is no waiting packet for this particular output port, and thus the probability that  $OPN_2$  will fire. We know the packets are waiting for ports that are busy, and thus all packets are for either this output port, or one of the other output ports that are free. The probability that a single packet can use this particular output is thus  $1/(6 - \#(FOP))$ . The probability that that packet cannot use this output port is  $(5 - \#(FOP))/(6 - \#(FOP))$ . If we have  $\#(WOP)$  waiting packets, then the probability that none of them can use the newly freed output port is

$$\left(\frac{5 - \#(FOP)}{6 - \#(FOP)}\right)^{\#(WOP)}$$

This, then, is the probability we assign to  $OPN_2$ ; we assign the complementary probability to  $OPY_2$ .

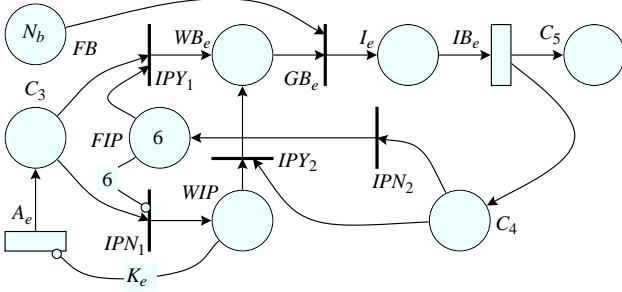


Figure 7: SPN subnet  $\mathcal{N}_3$ : packet transfer from a neighbor node to the current node.

**SPN subnet  $\mathcal{N}_3$**  is shown in Figure 7. Transition  $A_e$  generates the packets ready to be sent by neighbor nodes to the current node. This rate is simply the product of the processor injection rate  $\lambda$  and the average path length,  $\frac{2n-1}{3}$ , since the packet is injected into a new neighbor node for each hop it takes. The structure and internal arrangement of the third SPN subnet is similar to the second SPN subnet described above. Place  $FIP$  (analogous to  $FOP$ ) contains tokens corresponding to free input ports of the current node (with an initial marking of six tokens). For each waiting packet in place  $C_3$  (analogous to  $C_1$ ), there are two possibilities.

- If the required input port is available, immediate transition  $IPY_1$  (analogous to  $OPY_1$ ) fires and moves a token to place  $WB_e$ . Transition  $GB_e$  then reserves a buffer in the current node, if there is a buffer available. Transition  $IB_e$  completes the packet transfer, and the packet ends up in place  $C_5$  which is a place shared between the third and the fourth SPN subnets.

- If the required input port is busy, immediate transition  $IPN_1$  (analogous to  $OPN_1$ ) fires and moves a token to place  $WIP$  (analogous to  $WOP$ ) representing waiting packets. An inhibitor arc with cardinality six from  $FIP$  to  $IPN_1$  prevents transition  $IPN_1$  from firing when place  $FIP$  contains all six tokens.

A token in place  $C_4$  (analogous to  $C_2$ ) represents the state when a busy input port has just been released. As before, there are two possibilities:

- If there are no waiting requests for this input port, the immediate transition  $IPN_2$  will fire and return a token to place  $FIP$ .
- If place  $WIP$  has a packet waiting for this particular input port, the immediate transition  $IPY_2$  will fire and move a token in place  $WB_e$ .

The probabilities assigned to these cases are similar to those for  $\mathcal{N}_2$ , since the situation is analogous. An inhibitor arc with cardinality  $K_e$  from  $WIP$  to  $A_e$  is needed to ensure that the population of packets waiting to enter the current node from the neighbor nodes is finite. This introduces an approximation in our model, by truncating the state space.

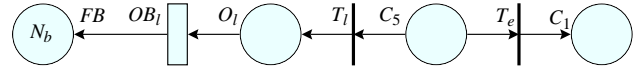
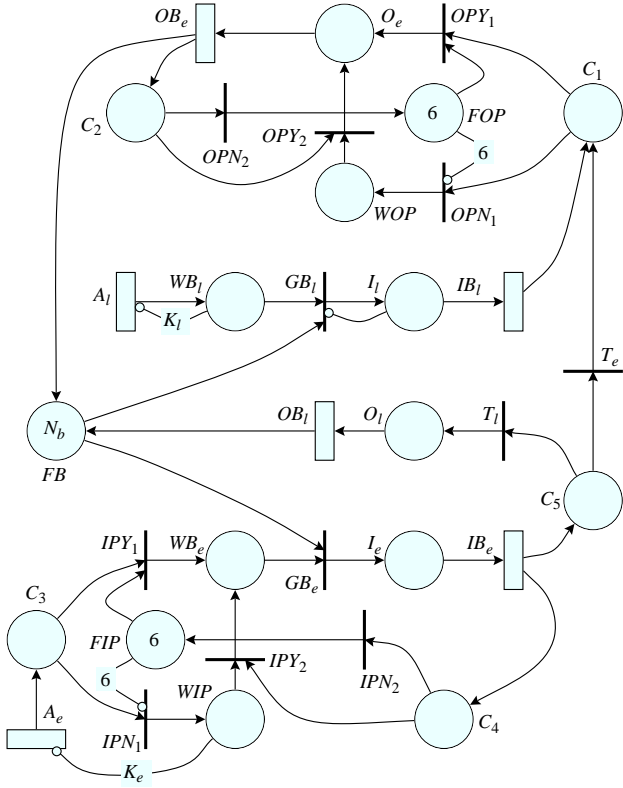


Figure 8: SPN subnet  $\mathcal{N}_4$ : packet ejection from the current node through the local processor port.

**SPN subnet  $\mathcal{N}_4$**  is shown in Figure 8. A token in place  $C_5$ , representing a packet received by the current node from its neighbors, is either destined to the current node, or must be transferred further.

- If the packet must be forwarded, then immediate transition  $T_e$  moves the token to place  $C_1$ , the input place of the second SPN subnet  $\mathcal{N}_2$ .
- If the packet must be ejected toward the local node, immediate transition  $T_l$  moves the token to place  $O_l$ . Transition  $OB_l$  represents the completion of the ejection, after which one buffer in the current node is released by returning a token to place  $FB$ . Note that the rate of transition  $OB_l$  is constant, not proportional to the number of tokens in place  $O_l$ , since the activity modeled corresponds to a “single server”.

The composite SPN net  $\mathcal{N}$  shown in Figure 9 is obtained as a superposition of  $\mathcal{N}_1$ ,  $\mathcal{N}_2$ ,  $\mathcal{N}_3$ , and  $\mathcal{N}_4$  by merging their shared places,  $FB$ ,  $C_1$  and  $C_5$ . The meaning of the places and transitions in this SPN is summarized in Table 1 and



$IPN_2$  is disabled if  $\#(FIP) = 5 \wedge \#(WIP) > 0$ .  
 $OPN_2$  is disabled if  $\#(FOP) = 5 \wedge \#(WOP) > 0$ .  
 $T_e$  is present only if  $n > 2$ .

Figure 9: Approximate SPN model  $\mathcal{N}$ .

the firing rate and probabilities of the transitions are given in Table 2. Note that places  $C_1, \dots, C_5$  are always empty in a tangible marking. Moreover, transition  $GB_e$  has priority over transition  $GB_l$ , to ensure that the delivery of packets in transit takes precedence over the injection of new packets into the network. A priority to local packets or an equal priority to local and external packets could also be easily modeled.

The inhibitor arcs with cardinality  $K_l$  and  $K_e$  from  $WB_l$  and  $WIP$  to  $A_l$  and  $A_e$ , respectively, introduce an approximation corresponding to a truncation of the state space. With exponentially distributed firing times, it is possible to have any number of packets waiting, but the probability of having many packets waiting decreases quickly unless the system is saturated. The introduced approximation does not influence the system behavior in the following two cases:

- If the system is lightly loaded, the probability of having more than a few waiting packets in places  $WB_l$  and  $WIP$  is close to zero. Hence, the effect of the

Transition	Firing rate	
$A_l$	$\lambda$	(an input parameter to be varied)
$IB_l$	$1/720 tu^{-1}$	
$OB_l$	$1/720 tu^{-1}$	
$A_e$	$(2n - 1)/3 \cdot \lambda$	
$IB_e$	$\#(I_e)/720 tu^{-1}$	
$OB_e$	$\#(O_e)/x$	( $x$ is the iteration parameter)
Transition	Priority	Firing probability
$IPY_1$	1	$\beta = \frac{\#(FIP)}{6}$
$IPN_1$	1	$1 - \beta$
$IPY_2$	2	$\gamma = 1 - \left( \frac{5 - \#(FIP)}{6 - \#(FIP)} \right)^{\#(WIP)}$
$IPN_2$	2	$1 - \gamma$
$T_l$	3	$\delta = \frac{3}{2n-1}$
$T_e$	3	$1 - \delta$
$OPY_1$	4	$\epsilon = \frac{\#(FOP)}{6}$
$OPN_1$	4	$1 - \epsilon$
$OPY_2$	5	$\phi = 1 - \left( \frac{5 - \#(FOP)}{6 - \#(FOP)} \right)^{\#(WOP)}$
$OPN_2$	5	$1 - \phi$
$GB_l$	6	1
$GB_e$	7	1

Table 2: Firing rates and probabilities of the transitions in the SPN  $\mathcal{N}$ .

introduced inhibitor arcs becomes negligible.

- If the system is saturated, even with the inhibitor arcs reducing the effective arrival rate, the probability of  $WB_l$  or  $WIP$  being nonempty is close to one. Increasing  $K_l$  or  $K_e$  only increases the state space and the solution cost, without changing in any appreciable way the numerical value computed for the throughput of packets.

The only undefined parameter in Table 2 is  $x$ , the average time required by an outgoing packet to obtain and fill a buffer in the next node on its path. Only after this time elapses can the buffer for node  $i$  be released (through the arc from  $OB_e$  to  $FB$ ). By symmetry, this time has the same average as the time that a packet in place  $WB_e$  must wait before it can obtain a local buffer slot and enter place  $I_e$ , plus the time to fill the slot,  $720 tu$ .

Hence, we set up the following fixed-point iteration scheme:

- Choose an initial guess  $x^{(0)}$  for  $x$ .
- Compute the successive values for  $x$  as  $x^{(i)} = w + 720 tu$ , where  $w$  is the average waiting time and is

Place	Meaning
$FB$	Free buffers.
$WB_l$	Locally generated packets, waiting for a buffer.
$I_l$	Locally generated packets, being copied into a buffer.
$O_l$	Packets destined to the local node, being copied out of a buffer.
$WB_e$	Externally generated packets, waiting for a buffer.
$I_e$	Externally generated packets, being copied into a buffer.
$O_e$	Packets destined to and external node, being copied out of a buffer.
$FIP$	Free input ports.
$FOP$	Free output ports.
$WIP$	Externally generated packets, waiting for an input port.
$WOP$	Packets to external node, waiting for an output port.
$C_1$	Choice: is the required output port available for the packet?
$C_2$	Choice: is there a packet waiting for the output port just released?
$C_3$	Choice: is the required input port available for an incoming packet?
$C_4$	Choice: is there a packet waiting for the input port just released?
$C_5$	Choice: is the local node the final destination for the packet?
Transition	Meaning
$A_l$	Locally generated packet is ready to be transmitted.
$GB_l$	Locally generated packet gets a buffer.
$IB_l$	Locally generated packet is put into a buffer.
$OB_l$	Packet directed to local node is read out of its buffer.
$A_e$	Externally generated packet is ready to enter the node.
$GB_e$	Externally generated packet gets a buffer.
$IB_e$	Externally generated packet is put into a buffer.
$OB_e$	Packet is transferred to an external node and frees its buffer.
$IPY_1$	Required input port is available.
$IPN_1$	Required input port is not available.
$IPY_2$	Input port just released is required by a packet waiting in $WIP$ .
$IPN_2$	Input port just released is not required by any packet waiting in $WIP$ .
$T_l$	Local node is the final destination for the packet.
$T_e$	Local node is not the final destination for the packet.
$OPY_1$	Required output port is available.
$OPN_1$	Required output port is not available.
$OPY_1$	Output port just released is required by a packet waiting in $WOP$ .
$OPN_2$	Output port just released is not required by any packet waiting in $WOP$ .

Table 1: Meaning of places and transitions in the SPN  $\mathcal{N}$ .

obtained using Little's law:

$$\begin{aligned}
 w &= \frac{E[\text{number of packets waiting}]}{E[\text{throughput of packets}]} \\
 &= \frac{E[\#(WIP) + \#(WB_e)]}{E[\text{rate}(A_e)]}
 \end{aligned}$$

- Stop the iterations when  $x^{(i)}$  and  $x^{(i+1)}$  are sufficiently close.

We conclude this section with an observation regarding the interaction between truncation and decomposition. If truncation were not required, we would expect that  $A_l$  and  $A_e$  (and the corresponding downstream transitions for the two, if the system is not saturated) would have throughputs

equal to their firing rates,  $\lambda$  and  $(2n-1)/3 \cdot \lambda$ , respectively. However, truncation causes the throughputs of  $A_l$  and  $A_e$  to be reduced. Since two parameters are needed,  $K_l$  and  $K_e$ , this requires some care.

The values of  $K_l$  and  $K_e$  affect the relative values of the two throughputs. We then ensure that the truncation does not force an incorrect behavior, by checking that, upon convergence of the fixed-point iteration, the ratio of the throughputs of  $A_l$  and  $A_e$  is “very close” to  $3/(2n-1)$ . If the ratio were smaller (larger) we could then increase (decrease) the value of  $K_l$  with respect to  $K_e$ . We did not experience this problem in practice, but it is important to be aware of the potential for error when applying both truncation of the state space and fixed-point iteration to the

same model.

## 5 Numerical results

In the numerical experiments, we considered systems of size  $E_3, \dots, E_8$ , with  $N_b = 10$  or 12, interarrival packet time  $1/\lambda = 1000 tu, 1100 tu, \dots, 2000 tu$ , and truncation parameters  $K_l = K_e = 3$ . In most cases, the fixed-point scheme converged in just a few iterations. For example, for  $E_5$ ,  $N_b = 12$ ,  $1/\lambda = 1200 tu$ , four iterations are needed, starting from the initial guess  $x^{(0)} = 1000 tu$ , to obtain four significant digits:  $x^{(1)} = 744.9 tu$ ,  $x^{(2)} = 729.3 tu$ , and  $x^{(3)} = x^{(4)} = 728.8 tu$ .

We discovered that the number of iterations increases as the the system is stressed, that is, as the mesh size increases, the number of buffers decreases, or the interarrival packet time decreases. The maximum number of iterations, thirteen, was observed for  $E_8$ , when  $N_b = 10$ , and  $1/\lambda = 1000 tu$ , resulting in  $x^{(13)} = 912.7 tu$ . Interestingly, this happens even if our initial guess,  $x^{(0)} = 1000 tu$ , turned out to be always an overestimate of the value obtained for  $x$  through the iterations, hence it is closest to the value  $x^{(13)} = 912.7 tu$  than to the final value of  $x$  obtained for any other combination of input parameters studied.

For our study, we focus on the **average total packet latency time**  $\tau$ , defined as the average time elapsing from the instant a packet is generated by its source local processor (firing of transition  $A_l$ ), to the instant it is read by its destination local processor (firing of transition  $O B_l$ ). In the model of Fig. 9, this is obtained as the sum of three components:

- The “injection time”: the average time a packet waits before it is put into a buffer in the source node, computed using Little’s law:

$$\frac{E[\#(W B_l) + \#(I_l)]}{E[\text{rate}(I B_l)]}$$

- The “ejection time”: the average time a packet waits before it is removed from the buffer in the destination node, computed using Little’s law:

$$\frac{E[\#(O_l)]}{E[\text{rate}(O B_l)]}$$

- The “transit time”: the average time a packet spends in transit, computed as the product of the time to perform a hop times the expected number of hops:

$$x \cdot \frac{2n - 1}{3}$$

Fig. 10 shows the value of  $\tau$  as a function of the average interarrival time  $\lambda^{-1}$ , for various system sizes ( $n$ ) and number of buffers ( $N_b$ ).

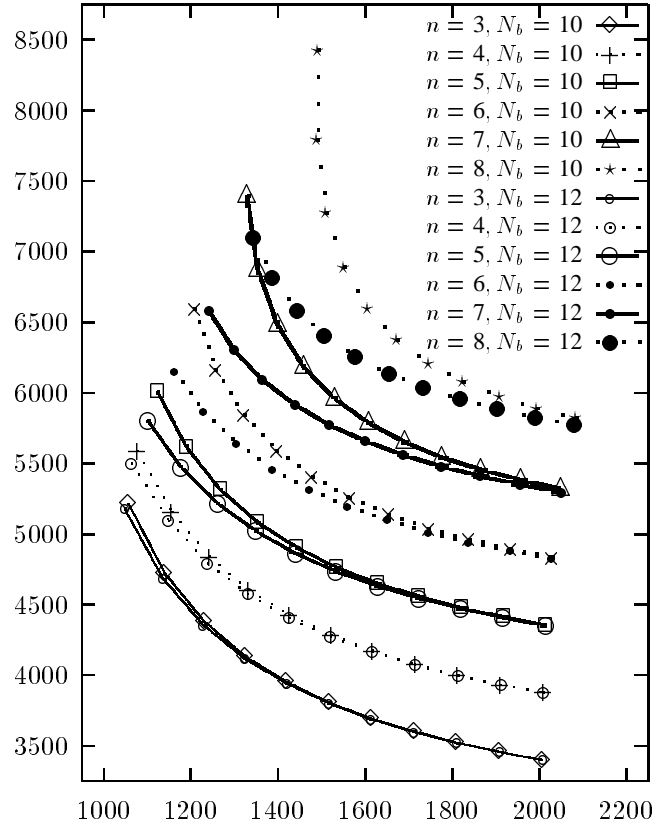


Figure 10: Latency  $\tau$  (in  $tu$ ) as a function of  $\lambda^{-1}$ , for different values of  $n$  and  $N_b$ .

## 6 Comparison with simulation results

In the real system, the time required to perform most activities is far from being exponentially distributed. With simulation, we can accurately portray any distribution, including exponential, uniform, or constant. For example, packet transfers into or out of buffers are constants of  $720 tu$  in the simulation model.

In a Markovian SPN, all time delay distributions are approximated with exponential distributions. By using Erlang distributions with the same mean, we better approximate the constant, or almost constant, nature of the random variables involved. Higher values of  $k$  result in better approximation, but they also increase the size of the state space.

With exponential distributions and  $N_b = 10$ , the underlying CTMC contains 32,797 nodes and 308,267 arcs. Increasing  $N_b$  to 12 results in 49,259 nodes and 476,838 arcs. Hence, we limited ourselves to check the effect of using Erlang(2) distributions. When using the Erlang(2) distribution for the  $N_b = 10$  case, the underlying CTMC contains 749,795 nodes and 6,829,308 arcs.

We constructed a simulation model capturing the essential architectural features of the interconnect. This simu-

lation model was built using the Design/CPN tool based on Hierarchical Colored Petri nets. All simulation runs involved over 500,000 packets, and the 95% confidence intervals using the batch means approach were tighter than  $\pm 1.1\%$ . For low traffic, the confidence intervals were significantly better than this.

The comparison of SPN model results (using either exponentially or Erlang(2) distributed times) against the simulation results is shown in Fig. 11 for the case of networks  $E_3$  and  $E_6$ , with  $N_b = 10$ . The percent workload, defined as  $\lambda \cdot 720 \cdot 100\%$  is on horizontal axis. In general, the results are off by only a few percent. As we would expect, the results with Erlang distributions agree with the simulation results much more closely. Interestingly, the results for a larger network show closer agreement than those for a small network. This is probably due to the fact that, under heavy load, the shape of the distribution of the interarrival times to the transitions is less important, since all transitions are more likely to be busy most of the time anyway.

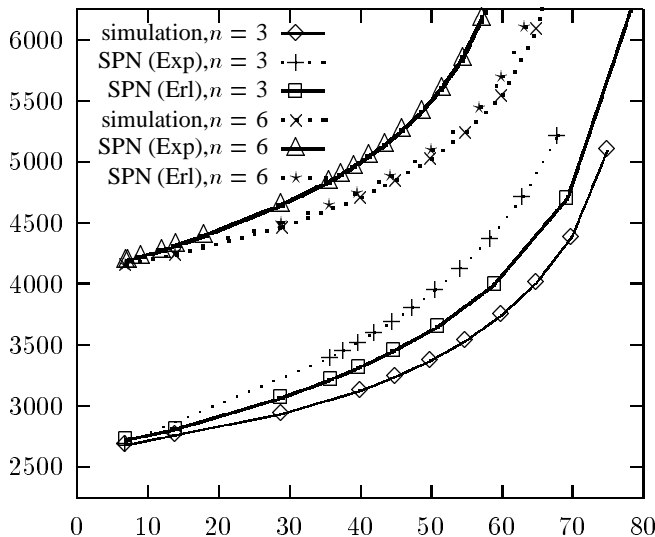


Figure 11: Comparison with simulation results: latency  $\tau$  (in  $tu$ ) vs. percent workload, for  $E_3$  and  $E_6$  ( $N_b = 10$ ).

## 7 Conclusion

We presented our experience in using SPNs to model an industrial size application. The paper has shown that SPN models can exploit the symmetry of the system to construct a tractable, but approximate, analytic model, and that they can yield results very close to those of a detailed simulation model, with much less computational effort.

One of the difficulties in using the SPNs is that all time delays are approximated with exponential distributions, while, in the real system, many time delays are constants. By using Erlang( $k$ ) distributions with a given mean in the SPN model, we can better approximate the constant

distribution. However, as we have seen, this can lead to a sharp increase in the size of the state space. To solve this problem, we are investigating the use of SPN having underlying discrete-time Markov chains [8, 2]. We are currently working on the design of a software package that will allow us to solve SPNs with continuous-time phase-type distributions, as those used in this paper, their discrete equivalent (where any distribution over the integers can be used, such as constant, discrete uniform, geometric or modified geometric), and even, under certain restrictions, with a mixture of the two (see the “deterministic and stochastic Petri nets” [1] and recent extensions [4]).

## References

- [1] M. Ajmone Marsan and G. Chiola. On Petri nets with deterministic and exponentially distributed firing times. In G. Rozenberg, editor, *Adv. in Petri Nets 1987, Lecture Notes in Computer Science 266*, pages 132–145. Springer-Verlag, 1987.
- [2] G. Ciardo. Discrete-time Markovian stochastic Petri nets. In W. J. Stewart, editor, *Numerical Solution of Markov Chains '95*, pages 339–358, Raleigh, NC, Jan. 1995.
- [3] G. Ciardo, A. Blakemore, P. F. J. Chimento, J. K. Muppala, and K. S. Trivedi. Automated generation and analysis of Markov reward models using Stochastic Reward Nets. In C. Meyer and R. J. Plemmons, editors, *Linear Algebra, Markov Chains, and Queueing Models*, volume 48 of *IMA Volumes in Mathematics and its Applications*, pages 145–191. Springer-Verlag, 1993.
- [4] G. Ciardo, R. German, and C. Lindemann. A characterization of the stochastic process underlying a stochastic Petri net. *IEEE Trans. Softw. Eng.*, 20(7):506–515, July 1994.
- [5] G. Ciardo and K. S. Trivedi. A decomposition approach for stochastic reward net models. *Perf. Eval.*, 18(1):37–59, 1993.
- [6] G. Ciardo, K. S. Trivedi, and J. Muppala. SPNP: stochastic Petri net package. In *Proc. 3rd Int. Workshop on Petri Nets and Performance Models (PNPM'89)*, pages 142–151, Kyoto, Japan, Dec. 1989. IEEE Computer Society Press.
- [7] K. Jensen. Coloured Petri nets. In *Petri Nets: Central Models and Their Properties LNCS*, vol. 254, pages 248–299. Springer-Verlag, 1987.
- [8] M. K. Molloy. Discrete time stochastic Petri nets. *IEEE Trans. Softw. Eng.*, 11(4):417–423, Apr. 1985.